Optimal Design of a Fully Superconducting Machine for 10-MW Offshore Wind Turbines

Thanatheepan Balachandran
Department of Elelctrical and Computer Engineering
University of Illnois at Urbana Champaign
Urbana, IL, U.S.A
tb8@illinois.edu

Dongsu Lee
Department of Elelctrical and Computer Engineering
University of Illnois at Urbana Champaign
Urbana, IL, U.S.A
dongsul@illinois.edu

Kiruba S. Haran
Department of Elelctrical and Computer Engineering
University of Illnois at Urbana Champaign
Urbana, IL, U.S.A
kharan@illinois.edu

***Abstract*— Fully superconducting (SC) machines hold immense promise for high-power-density and higher efficiency machine solutions for offshore wind turbine applications. In this paper, a 10MW air-core fully SC machine is designed for offshore wind turbine applications. This machine design is considered with inside armature coils and outside rotating field coils. In this topology, shield iron can be eliminated or reduced by replacing it with shield coils which contain the magnetic flux inside the machine. This machine is attractive for off-shore wind turbine application due to its high-power density and high efficiency compared to a conventional shield iron design. However, due to the introduction of additional shield coils, this topology uses relatively more amount of SC material than a conventional shield iron design. Therefore, a tradeoff between the shield coils and the shield iron is explored in this paper. In addition, machine designs with different pole-counts are investigated to identify the optimal pole-count design for a low-speed application. A detailed ac loss calculation is evaluated for the machine and required cryocooler power is evaluated to obtain the machine efficiency.**

Keywords— Air-core machines, Fully superconducting machines, High-power density, Offshore wind turbine, Optimal machine design

I. INTRODUCTION

Superconducting machines have been proposed and demonstrated for several high-power-density applications such as wind turbines, electric aircraft, and ship propulsion. Most of these machines are partially SC; they consist of conventional armature coils made of copper or aluminum, and SC field coils made of SC materials such as Magnesium diboride (MgB_2), Niobium–tin (Nb_3Sn) or Yttrium barium copper oxide (YBCO). A fully SC machine topology uses superconductors in both the armature and field coils. Compared to a fully SC machine, partially SC machines are attractive due to their stationary SC field coils which have the advantage of simplified machine construction and associated cryocooler designs. However, fully SC machine can further improve the machine power density by pushing the armature current density.

Under dc condition, SC materials exhibit no losses, but ac losses occur in the windings when ac current and field are introduced. Ac losses are cyclic and thus increase with the operating electrical frequency. These losses in the fully SC armature coils are difficult to manage and pose a significant barrier in relatively high-frequency machines such as those used in electric aircraft propulsion. But, low frequency wind turbines are an attractive application for fully SC machines. Core loss is another challenge of SC machine due to the higher magnetic fields generated by SC field coils. Higher fields saturate the iron core and limit the achievable air-gap flux density. Therefore, a complete air-core SC machine design with an inside-out synchronous generator configuration is proposed to eliminate the core loss and open up a design space with a higher air-gap flux density [1]. In this topology, the traditional shield iron is replaced with shield coils for containing the magnetic flux within the machine. This topology was explored under a National Aeronautics and Space Administration (NASA) LEARN program, showing significantly improved power density in aerospace applications.

In this work, actively shielded fully SC machine topology is considered for a wind turbine application. An abstract 3-D model of actively shielded and iron-shield design is shown in Fig. 1.

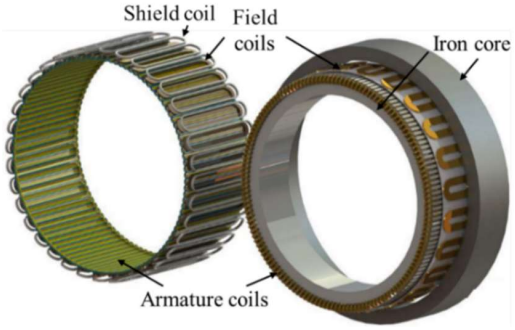

Fig. 1. Air-core architecture with shielding coils (Left: air-core SC machine, Right: iron-core SC machine) [2].

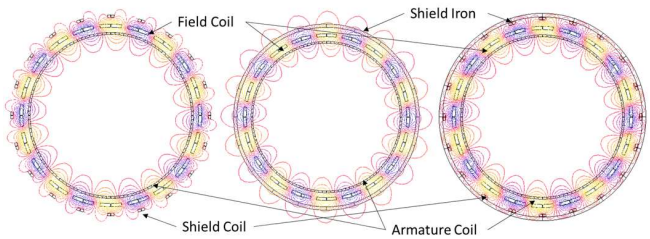

Fig. 2. Comparison of magnatic flux line of shield-coil, shield-iron and combined (shield-coil and shield-iron) designs.

Actively shielded coils contain the magnetic flux within the machine without significant change in airgap flux density. Fig.2 presents a comparison of flux density variation in the airgap and outside the machine for these three different machine topologies. However, increase in SC usage and associated cost is a drawback of the design. Reintroducing iron-shield to this topology may reduce the SC usage. Since the machine has outside field coils, iron shield acts as the magnetic core and increases the flux density in machine. This reduces the SC usage, but increases the machine weight. In this study, a tradeoff between shield iron and shield coil is investigated. A multi-objective optimal machine design is performed to obtain an optimum cost and weight machine while achieving the targeted ac losses. This paper is organized as follows, Section II summarizes the previous studies conducted on air-core actively shielded fully SC machines. Section III provides the specifications of the targeted machine, Section IV summarizes the ac loss models used to evaluate machine ac losses. Section V describes the optimal design scheme. Section VI gives the simulation results and analysis. Finally, Sections VII and VIII presents the proposed mechanical design and concluding remarks.

II. Actively Shielded Superconducting Machines

The air-core actively shielded fully SC machine topology uses shield coils which are introduced radially outward from the field coil to cancel the magnetic flux outside the machine. The key to the design is the elimination of iron shield and iron core. This achieves a higher power density by pushing the air-gap flux density to three to five times that of a conventional machine. Machine efficiency is increased by eliminating core losses and minimizing copper losses. The result shows higher efficiency even with the cryogenic cooling power considered. Initial EM studies on actively shielded fully air-core SC machines showed higher field strength, up to 10T is realizable with 99% efficiency. Previous studies focused on high frequency machines showed that, compared to a conventional iron-shield design, a 35% diameter reduction with a corresponding weight reduction could be achieved through 17% more SC usage compared to a conventional iron-shield design [1]. Another multi-objective optimization study showed that a 32% of volume reduction can be achieved by a 33% more SC [3]. A pole-count study to obtain optimal design to make the machine more compact, showed that a 74% volume reduction can be obtained with a 104% more superconductor usage. A 10-MW 3000 rpm electric machine is proposed for electric propulsion. The pole-count is changed from 6 to 18 with appropriate machine parameter modification. Results showed a lower pole-count design allows volume reduction and heat losses. An 8-pole design showed better performance in terms of flux density, effective shielding, and a small enclosure radius [4].

An analytical ac-loss study of a similar machine with fully SC and partial SC configurations is performed in [5]. Results showed that a fully SC machine with MgB_2 armature coils had 580W ac losses. This is smaller than the other MW range machines proposed in the literature. Most of these studies are focused on high-speed applications such as electric propulsion. However, these preliminary results show that this topology will be a good candidate for wind turbines. In our previous study, this topology is explored for wind turbine applications [2]. A 40-pole machine design is studied, and performance of the generator is analyzed in terms of torque production, ac loss and impact of shield coils.

The active shield topology enables the consideration of low-pole-count designs, which reduces the ac losses in the SC armature coils, thus making it suitable for wind turbine applications. This study focuses on obtaining an optimal design of various pole-count machines in term of weight and cost. This study reveals how shield iron contributes to the weight as well as how machine power density can be increased at the expense of more SC usage. Performances are obtained using finite element analysis (FEA) for better accuracy. Results are compared with respective baseline model in terms of ac loss, flux density, torque density, cost and volume, etc. The optimized design is used to validate the air-core design topology for offshore wind turbine applications.

III. Proposed Fully SC Machine

In this study a 10-MW, 10 rpm, fully SC air core machine for wind turbine generator is considered. Specifications of the targeted 10-MW SC machine considered in this study are given in Table I. Multifilament MgB_2 SC wires are chosen for the armature winding due to their low ac loss characteristics. Specifications of the chosen MgB_2 wires tabulated in Table II, are used in the ac loss calculation and total SC volume calculation. Since the machine is used as a direct-drive offshore wind turbine, 10 rpm is considered as the machine speed. Machines with various number of poles are considered, while an optimal design for each pole design is explored. A comparison table is provided to identify the pole count which corresponds to low ac-losses.

TABLE I. Proposed Machine Specifications

Specification	Value
Power	10MW
Pole number	10 / 20 / 36 / 60
Speed	10 rpm
Superconductor	MgB_2
Operating temperature	20 K
Armature Current density at 2T	140 A/mm^2
Field current density at 2T	200 A/mm^2
Shield current density at 2T	200 A/mm^2

TABLE II. MgB_2 Conductor Data

Symbol	Parameter	Conductor I 0.85/44/10 Armature	Conductor II 0.85/28/5 Field and Shield
J_c	Critical current density at self-field at 20K [A/m^2]	1.78e9	1.78e9
R_0	SC diameter [mm]	0.85	0.85
a	Filament diameter [mm]	0.044	0.028
n	Number of filaments	54	114
λ	The area fraction of the wire that is SC	0.15	0.15
α	The wire's internal eddy current shielding factor	0.7	0.7
ρ_e	Effective transverse resistivity [Ω-m]	2.3e-8	2.3e-8
L	The twist pitch	0.01	0.005

This work was supported in part by the National Science Foundation under award No 1807823.

The torque profile and ac losses are evaluated and compared with those of similar 10-MW, 10 rpm, fully SC machines proposed in literature

IV. AC Loss Evaluation

Losses will occur in the SC material and create heat when alternating current and fields are introduced. These losses are a form of hysteresis loss and can be modeled macroscopically as well as microscopically. Fully SC machines armature windings experience both the alternating transport current and field, thus generating heat in the windings. Because SC windings are to be kept under critical temperature at operating condition, this heat needs to be removed from the windings to avoid quenching. Most of the fully SC machine designs in the literature are primarily focused on EM designs and validating their electrical performance. However, practical implementation of these machine designs depends heavily on accuracy of estimated ac losses and associated cryocooler design.

In this study, ac losses in the armature windings are evaluated using Wilson's model proposed in [6]. This approach is widely adopted in literature [7]-[8] to evaluate ac losses in fully SC machines. First, ac losses across the unit length of multiple SC conductors are evaluated to identify a low ac loss MgB2 conductor. Selected conductor's ac losses are compared at the operating condition tabulated in Table III at various frequencies. The applied field is assumed to be uniform across the wire conductor area and the losses are evaluated. Estimated total ac loss for both the conductors using Wilson's model is shown in Fig. 3. The differences in estimated losses for different conductors are significant and increase at higher frequencies. Therefore, a lower ac-loss conductor II is selected for the armature, while selecting the conductor I for field winding.

TABLE III. Assumed Operating Condition

Operating condition parameters	Value
Field	2T
Temperature	20K
Critical Current Density	1.78×10^9 A/m^2
Critical current ($\boldsymbol{I_c}$)	150A
Operating Current ($\boldsymbol{I_{op}}$)	75A

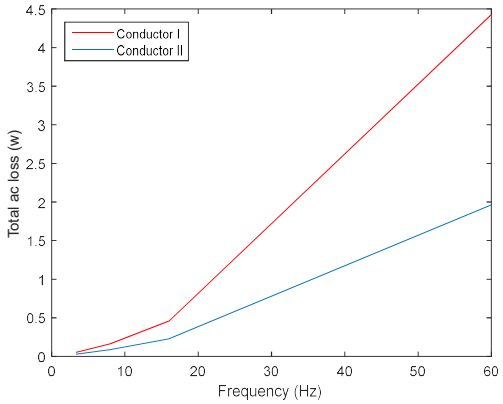

Fig. 3. Comparison of total loss (W) vs Frequency (Hz) evaluated using Wilson's models for choosen conductors.

Then, the same ac loss models are used to evaluate the ac losses in a unit length of armature winding and integrating over the total length to evaluate the total loss. Since the flux density at various points across a given armature slot is different, ac losses are evaluated by dividing the armature slot in to three equal areas as shown in the Fig. 4. Flux density at each region is evaluated using FEA and associated ac losses are calculated for each area separately. A ratio of 1:100 is used to size the required cryocooler power. For example, to remove 1 W of ac loss from the armature winding, 100 W of cryocooler power is needed. Other losses such as radiation and conduction loss also need to be incorporated for a complete efficiency calculation.

V. Optimal Design Sheme

A simulation-based approach is chosen to explore the optimal design. The objective function is formulated as (*1a*) - (*1g*) to minimize the cost and weight. The cost and weight of the machine is minimized using the total SC usage and shield-iron usage in the machine:

$$\underset{\theta=variabl\ \ set}{Minimize}\ F_{objective}(\theta) = [Cost, Weight] \quad (1a)$$

$$s.t\ P_{out} = 10MW \quad (1b)$$

$$Machine\ radius < 2.2m \quad (1c)$$

$$Outside\ flux\ density < 1mT \quad (1d)$$

$$Machine\ axial\ length < 5m \quad (1e)$$

$$Total\ ac\ loss < 3kW \quad (1f)$$

$$J_a < \frac{I_c}{2}\ Evaluated\ at\ armature\ flux\ density \quad (1g)$$

The cost and weight of the machine is evaluated from (*2*) - (*6*):

$$SC_v = SC_{a\_A} * (l_M + l_{e\_A}) + SC_{a\_F} * (l_M + l_{e\_F}) + SC_{a\_S} * (l_M + l_{e\_S}) \quad (2)$$

$$SI_v = SI_a * l_M \quad (3)$$

$$Weight = \rho_{SC} * SC_v + \rho_{SI} * SI_v + K_w \quad (4)$$

$$SC_l = \frac{SC_{a\_A}}{\pi R_0^2/4} * (l_M + l_{e\_A}) + \frac{SC_{a\_F}}{\pi R_0^2/4} * (l_M + l_{e\_F}) + \frac{SC_{a\_S}}{\pi R_0^2/4} * (l_M + l_{e\_S}) \quad (5)$$

$$Cost = SC_{up} * SC_l + SI_{up} * SI_v + K_c \quad (6)$$

where SC_v is the total SC volume used in the machine, SC_l is the total length of SC wire used in the machine and SI_v is the total shield-iron volume used in the machine. SC_{up} and SI_{up} are unit prices of SC and shield-iron, ρ_{SC} (8,250 kg/m^3) and ρ_{SI} (8,250 kg/m^3) are the density of SC and shield-iron respectively. For the cost evaluation, SC wire tabulated in table II is priced as \$2/m and shield iron price is considered as \$2/kg. K_c is the fixed additional cost associated with the machine and K_w is the fixed additional weight. SC_{a_A}, SC_{a_F} SC_{a_S} are cross sections of armature, field and shield slots respectively; similarly l_{e_A}, l_{e_F}, l_{e_S} are the end-winding lengths; SI_a is the shield-iron cross-section area; R_0 is the SC wire diameter and l_M is the active

generator length calculated to satisfy the rated torque. Axial length is calculated as:

$$l_M = \frac{T^e_{rated}}{T^e} \quad (7)$$

where T^e_{rated} is the rated torque of the targeted machine and T^e is the average torque obtained from FEA for a candidate machine. Optimization is performed by changing the design parameters to obtain candidate machine designs. When $SI_v \gg SC_v$, machine cost is minimized at the expense of greater weight. When $SI_v \ll SC_v$, machine weight is minimized, thus providing designs which are better suited to offshore wind turbine. But this comes at the expense of higher cost. When $SC_v \approx SI_v$, designs which optimize both weight and cost can be obtained.

Fig. 4 shows the configurations and nine design variables used for optimal machine design. An evolutionary genetic algorithm (GA), GOSET (an opensource MATLAB toolbox) was specifically chosen to optimize the machine design [9]. The optimization is allowed to operate within the design space:

$$\theta = [X_1, X_2, X_3, X_4, X_5, X_6, X_7, X_8, X_9] \quad (8)$$

Design boundary considered for each variable is tabulated in Table IV. Design variable X_5 and X_7 are functions of machine pole-count. When the pole-count changes, these ranges are changed proportionally. For a 36 pole-count design, maximum limit of X_5 is set to be 3.8º degrees while the limit of X_7 is set to be 40 mm. The flowchart of the optimal design process is shown in Fig. 5. The optimization process begins by the GA generating candidate variables within the range given in Table IV. These variables are used in FEA to model the machine. Based on FEA, characteristics such as torque and flux density at pre-defined paths are obtained. From these results, axial length, cost, and ac losses are calculated by an analytical method. Then ac loss, maximum machine radius, axial length and leakage flux density are compared with the constraint values; if all constraints are satisfied, then the design is considered valid.

The fitness function for the GA is given by:

$$F_{fitness}(\theta) = [\frac{1}{Cost}, \frac{1}{Weight}] \quad (9)$$

The GA is then used to maximize the fitness which will minimize machine weight and SC usage. This process is repeated for various pole-count designs to identify the best pole-count design for a low-speed application. Since part of the design problem is to obtain a low ac-loss model while minimizing the weight and SC usage, constraints are placed for ac losses on each pole-count designs. For example, for a 20 pole-count design, 3 kW is chosen as the limit. As the GA evolve towards optimal design, designs with large ac losses are eliminated from the population.

Similarly, the outside flux density limit is chosen to be 1mT at a distance of 10 mm from the shield iron while machine radius and axial length are limited at 2.2 m and 5 m respectively for all the pole-count designs.

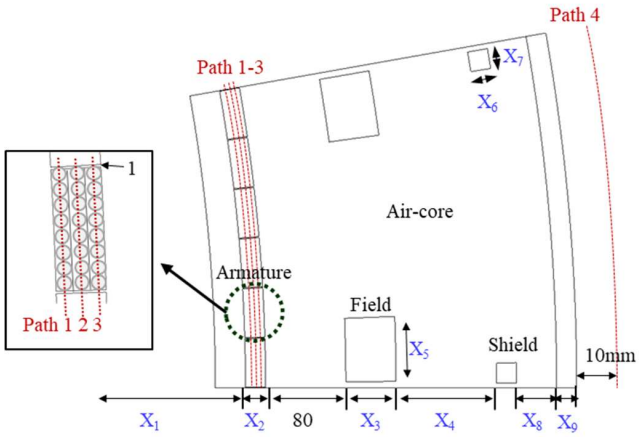

Fig. 4. Configurations and design variables of the SC machine

TABLE IV. DESIGN BOUNDARIES

Variables	Minimum	Maximum
X1 [mm]	1,600	2,000
X2 [mm]	10	100
X3 [mm]	50	100
X4 [mm]	20	100
X5 [Angle]	1	$f(P)$
X6 [mm]	1	100
X7 [mm]	1	$f(P)$
X8 [mm]	1	100
X9 [mm]	1	100

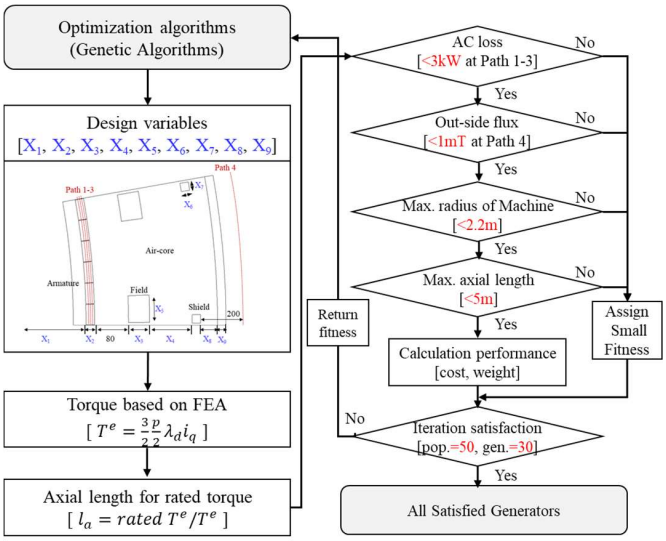

Fig. 5. Flowchart of the optimization process

Machine designs which violate these constraints are eliminated from the population by assigning small fitness values. In this optimization process, a group of 300 generators is chosen as the initial population. Then, 50 machine designs are generated over 30 generations in GA to identify the best performance machines.

VI. Results

All the 20-pole generators satisfied the constraints that are shown in Fig. 6. The Pareto-front achieved within this population is shown in Fig 7. This reveals the best achievable tradeoff between cost and weight, while satisfying all the constraints. The machine weight can be reduced 2 to 3 times by increasing the size of the shield coils. However, this increases the machine cost by 30-50%. Fig. 8 gives a comparison of 20-pole machine SC volume against the SI volume. Results show that reducing the shield iron will increase the SC usage, which will increase the machine cost. Evaluated minimum and maximum ac losses for each pole-count generator are tabulated in Table V. A comparison between different pole-count designs generated in this optimization study showed that 20-pole count generator uses the minimum weight of SC. Since other pole-counts (10,36,60) did not converge within the generated population, the results for these pole-count machines are not reported in this work.

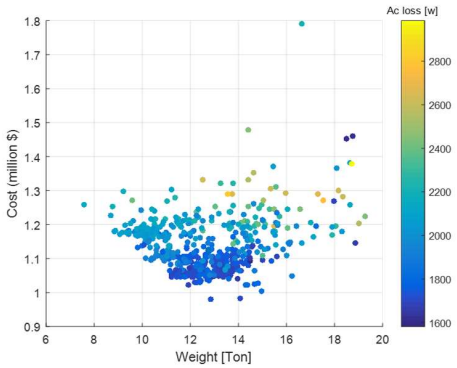

Fig. 6. All satisfied generators for 20 pole machines

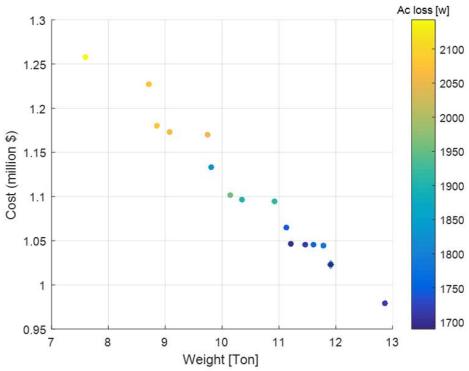

Fig. 7. Pareto-front for 20-pole machine

TABLE V. AC Loss and Efficency

Pole-Count	Minimum ac loss (kW)	Maximum ac loss (kW)	Required minimum cryocooler power (kw)	Achievable maximum efficiency (%)
10	1.40	2.98	140	98.59
20	1.58	2.95	158	98.40
36	1.89	3.00	188	98.09
60	4.63	4.98	463	95.32

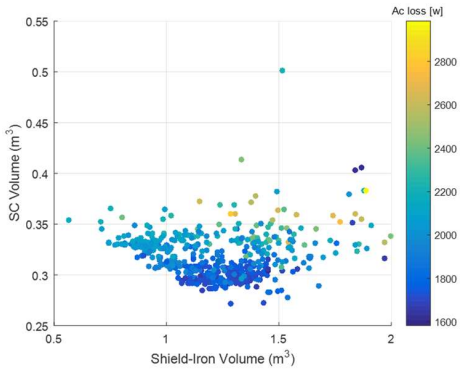

Fig. 8. SC volume and Shield Iron volume variation for 20-pole machines

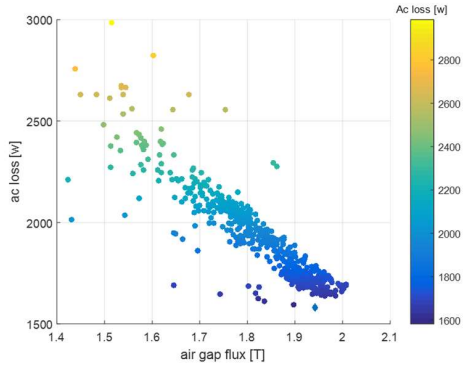

Fig. 9. AC loss and air-gap flux density variation for 20-Pole machines

Fig. 9 presents the ac-loss variation against airgap flux density evaluated for 20-pole machines. Results show that the achievable minimum total ac loss decreases with increasing airgap flux density. Required torque under higher air-gap flux density can be achieved using a shorter axial length, which reduces the SC usage in the armature, thus generating lower ac losses. However, as the airgap flux density increases, armature current needs to be decreased to give a safety margin to avoid quenching. On the other hand, when the air-gap flux density decreases, armature current can be increased to compensate the decrease in air-gap flux density. This method needs an iterative process to optimize the armature current. In this study armature current density is fixed to be half of the critical current evaluated at air-gap flux density. The machines violate these criteria are eliminated from the population.

Comparison of FEA results of the optimized model magnetic flux density are shown in Fig.10. This shows two 20-pole machine designs with a lower weight and lower cost. It is evident that iron shield and shield coils are compensating each other to reduce the flux density outside the machine to a required level. Fig. 11 shows the comparison of flux density distribution of a baseline model and an optimized 20-pole machine. Optimized model increases the air-gap flux density by optimizing the machine parameters. Therefore, required output torque is achieved by decreasing machine axial length. Total SC usage of the optimized model is reduced by 34.63% compared to the baseline model. A weight reduction of 29.72% and cost reduction of 33.68% is also achieved.

TABLE VI. COMPARISON OF MACHINE PARAMETER OF BASELINE MODEL AND OPTIMIZED MODEL

Machine Parameter	Base Model	Optimized Mode
Armature ID (x_1) [mm]	1047.0	1488.5
Armature slot height (x_2) [mm]	21.6	26.85
Distance between field and shield coils (x_3) [mm]	55.6	74.9
Field slot height (x_4) [mm]	73.3	90.2
Field slot width (x_5) [Degree]	4.23	2.3
Shield slot height (x_6) [mm]	38.8	37.7
Shield slot width (x_7) [mm]	58.6	38.6
Shield-iron thickness (x_8) [mm]	85.3	116.7
Distance between shield coil and shield-Iron (x_9) [mm]	5.7	4.8
Machine radius [mm]	1,408	1920
Machine axial length [mm]	1,649	639
Airgap flux density [T]	1.74	1.92
Outside flux density [mT]	0.01	0.001
Armature volume [m^3]	0.145	0.15
Field volume [m^3]	0.249	0.13
Shield volume [m^3]	0.091	0.034
SC volume [m^3]	0.485	0.317
Shield-iron volume [m^3]	1.207	0.872
Total loss [w]	2,626	1819
Armature SC wire length [km]	205	141
Total SC wire length [km]	855	560
Weight [Ton]	13.96	9.81
Cost [million$]	1.731	1.13

A detail comparison between baseline model and optimized model is provided in Table VI. This can be further improved by considering larger populations and a higher number of generations in GA.

VII. MECHANICAL DESIGN

The rotor and stator assemblies of the proposed machine are mechanically and thermally independent as proposed in [10]. An inside-out synchronous machine topology will be adopted, where dc excitation poles are located on the outside rotor and ac armature winding are located in the inside stator. A king-pin nacelle integration has been proposed in [11] by mounting the generator in front of the blades. Key features of this design include field windings fixed to the stationary king pin while the armature is connected to the rotating hub. Both simplify the cryogenic design. Since full power is transferred to the grid using slip rings, it is suggested that an outer rotor configuration is beneficial. This nacelle integration will be investigated for the proposed machine. Once the EM design is validated, a mechanical performance will be investigated.

VIII. CONCULSION AND FUTURE WORK

An optimal design of a 10-MW 10 rpm air-core, fully SC machine for an offshore wind turbine application is investigated in this paper. Optimized machine design is obtained to minimize the weight and cost of the machine while achieving targeted ac losses and machine size. A population of 50 machines over 30 generations is considered for each pole-count design to obtain an optimal design. All the satisfied generators obtained from the optimization of 20-pole machine designs are provided in this paper. A tradeoff between the cost and the weight is explored and results are provided. In future work, an optimal design for every pole count will be investigated by increasing the population. Further, Pareto optimal front for each pole count will be obtained to give more insight in to the achievable trade-off between the weight and the cost. Further, machine models which minimize ac loss also will be explored.

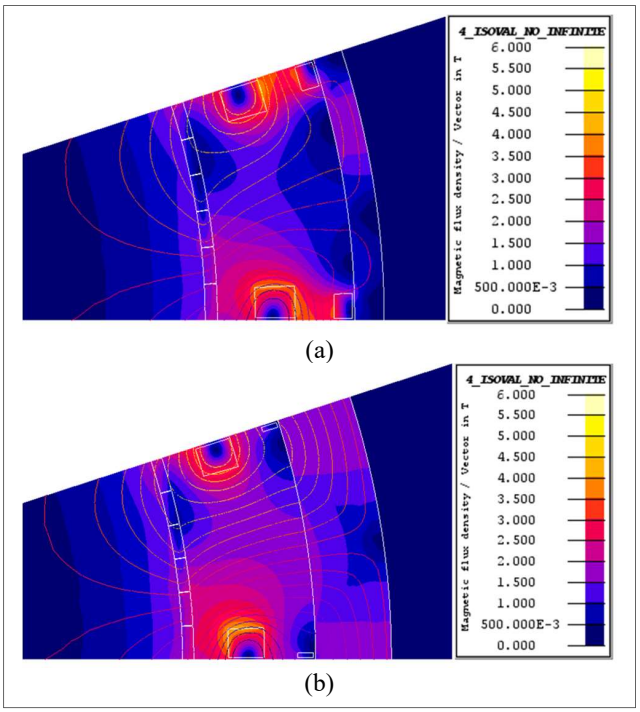

Fig. 10. Flux denisty distribution of a 20-pole machine design (a) low-weight (high-cost) design and (b) high-weight (low-cost) design.

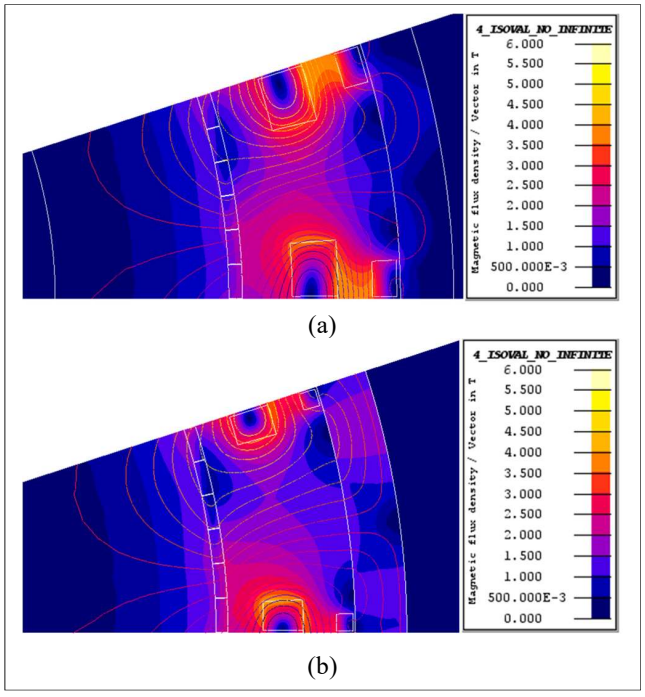

Fig. 11. Flux density distribution of 20-pole (a) baseline model and (b) optimized model.

A comparison between baseline model and optimized model is used to evaluate the efficiency of the optimization technique used. Results show that the optimized model has good performance compared to the baseline model while minimizing the cost and weight significantly. The results also show that the performance of this generator is similar to other MW range machines available in the literature in terms of size and ac losses. This optimized model will be used to design 3D models for mechanical validation of this machine.

REFERENCES

[1] K. S. Haran, D. Loder, T. O. Deppen and L. Zheng, "Actively Shielded High-Field Air-Core Superconducting Machines," IEEE Trans. Appl. Supercond., vol. 26, no. 2, pp. 98-105, Mar. 2016, Art no. 5202508.

[2] Dongsu Lee, T.Balachandran, Kiruba S.Haran, "Exploring Fully Superconducting Air-Core Machine Topology for Off-shore Wind Turbine Applications," Joint MMM-Intermag Conference, Washington, DC, USA, 2019.

[3] D. C. Loder and K. S. Haran, "Multi-objective optimization of an actively shielded superconducting field winding," 2015 IEEE Power and Energy Conference at Illinois (PECI), Champaign, IL, 2015, pp. 1-4.

[4] D. C. Loder and K. S. Haran, "Multi-objective optimization of an actively shielded superconducting field winding: Pole-count study," 2015 IEEE International Electric Machines & Drives Conference (IEMDC), Coeur d'Alene, ID, 2015, pp. 1709-1714.

[5] M. Fedderson, K. S. Haran and F. Berg, "Analytical ac loss study of MgB2-based fully superconducting machines," IOP Conference Series: Materials Science and Engineering, vol. 279, no. 1, pp. 12-26, 2017.

[6] M. Wilson, Superconducting Magnets. Clarendon Press Oxford, 1983.

[7] A. Kostopoulos, Dimitris Liu, Dong Genani, Gaurav & Polinder, Henk, "Feasibility Study of a 10 MW MgB2 Fully Superconducting Generator for Offshore Wind Turbines," EWEA Offshore 2013, Frankfurt, Germany, 19-21 November 2013.

[8] F. Lin, R. Qu, D. Li, Y. Cheng and J. Sun, "Electromagnetic Design of 13.2 MW Fully Superconducting Machine," IEEE Trans. Appl. Supercond., vol. 28, no. 3, pp. 1-5, April 2018, Art no. 5205905.

[9] S.D. Sudhoff, Optimization-Based Design, in Power Magnetic Devices: A Multi-Objective Design Approach. Hoboken, New Jersey: Wiley, 2014.

[10] S. S. Kalsi, "Superconducting Wind Turbine Generator Employing MgB2 Windings Both on Rotor and Stator," IEEE Trans. Appl. Supercond., vol. 24, no. 1, pp. 47-53, Feb. 2014, Art no. 5201907.

[11] A. B. Abrahamsen, N. Magnusson, D. Liu, E. Stehouwer, B. Hendriks and H. Polinder, "Design study of a 10 MW MgB2 superconductor direct drive wind turbine generator," Proceedings of EWEA, 2014.